

NEAR-FIELD IMAGING OF THE MICROWAVE DIELECTRIC PROPERTIES OF SINGLE-CRYSTAL PbTiO_3 AND THIN-FILM $\text{Sr}_{1-x}\text{Ba}_x\text{TiO}_3$

Y.G. WANG^a, M.E. REEVES^{a,b}, W. CHANG^b, J.S. HORWITZ^b and W. KIM^b

a Department of Physics, The George Washington University, Washington, DC, 20052

b Naval Research Laboratory, Washington, DC, 20375

ABSTRACT

A PbTiO_3 crystal and $\text{Sr}_{1-x}\text{Ba}_x\text{TiO}_3$ films have been studied by near-field scanning microwave microscopy (SMM). In the PbTiO_3 crystal, dielectric properties and topography are obtained simultaneously. In $\text{Sr}_{1-x}\text{Ba}_x\text{TiO}_3$ films, local variations and sample-to-sample differences are observed. To quantitatively determine local dielectric permittivity and loss, we also carry out theoretical calculations on dependence of resonant frequency and quality factor on dielectric constants of bulk samples and thin films. Good agreements between experimental and theoretical results are obtained.

I. INTRODUCTION

With the rapid progress in communication technology and growing demand for high permittivity materials, microscopic characterization of dielectric materials in GHz frequency range has become more important. So far, several types of near-field scanning microwave microscopies (SMM) have been developed, including $\lambda/4$ resonator, [1] coaxial line, [2] ring resonator [3], and submicron resolutions have been achieved. However, it is still a challenge to quantitatively characterize the microwave properties on a microscopic scale because the Coulomb force between the tip and sample depends not only on the material properties, but also on geometric factors of tip, sample and experimental setup.

In this paper, we report both our experimental and theoretical approaches to characterize dielectric properties by SMM using a $\lambda/4$ resonator [1]. We obtain the dependence of the local dielectric permittivity on the measured resonant frequency, f_0 , of the cavity under various conditions. In particular, we find both experimentally and theoretically that the measured df_0/dz is a linear function of the material dielectric constant, ϵ , when ϵ is high enough. Topographic features also contribute to the measured signal. We are able to distinguish the topographic contribution to the electrical response by adjusting the position of the tip accurately in measurements of a PbTiO_3 crystal.

II. EXPERIMENTAL AND THEORETICAL APPROACHES

The SMM used in our study mainly consists of a $\lambda/4$ coaxial resonator [1] with a resonant frequency about 1.75 GHz and an HP 8753D network analyzer. The $\lambda/4$ resonator is shown in the inset of Fig.1. A bottom metal plate is attached to the cavity so that the electric field is strongest at the end of the central conductor. A tungsten STM tip protrudes from the central conductor of the cavity and comes close to samples under study. Thus near-field microscopy in the submicron range can be realized. To accurately control the position of the tip in three dimensions, piezoelectric actuators are used to position the sample.

For comparison with experiments, we perform finite-element calculations on the electromagnetic fields inside the cavity and of the tip-sample assembly. When calculating the field near the tip, a static approximation is used considering that tip size is much smaller than the wavelength (17 cm at 1.75 GHz). The tip, consisting of a cylinder and a cone with a spherical end, is assumed to hold a constant potential. The cylindrical symmetry further simplifies the solution so that the electric field near tip can be obtained by solving the Poisson's equation $\nabla^2\phi=0$ in two-dimensions. To be consistent with experiments, a metal ground plane is added below the sample. The changes of resonant frequency and Q are then obtained using perturbation theory. That is, we assume that the small contribution of the fields generated within the sample are capacitively coupled to the cavity.

III. RESULTS AND DISCUSSION

First, we calculated the electric and magnetic fields inside the cavity. It is found the electric field is strongest at the open end of the central conductor where the STM tip is incorporated. On the contrary, the magnetic field is zero here. A bottom metal plate closes the cavity, effectively concentrating the electric field near the tip, reducing the resonant frequency. This result agrees with our experimental observation.

The calculated resonant frequency is further decreased by incorporating the tip into the cavity. This has been confirmed experimentally by using tips of various length. We also calculate the sensitivity to changing dielectric properties and the spatial resolution for various tip sizes. It is found that decreasing the tip radius decreases the sensitivity of the system but increases the spatial resolution.

Calculations of changes in f_0 and Q with distance z between tip and samples with different dielectric constants show excellent consistency to the corresponding experimental observations. It is interesting to note that the derivative of resonant frequency with tip-sample distance, df_0/dz , increases linearly with the dielectric constant, ϵ , when $\epsilon > 10$. Both the theoretical calculations and the experimental measurements exhibit the ten-

gency shown in Figure 1. This is quite important because most materials interesting for microwave applications have dielectric constants within this linear range. By our method, we are able to determine the dielectric properties more accurately irrespective of the effects of sample size and shape. In general, the resonant frequency is expected to change with the size of the sample under study due to the long-range character of Coulomb interactions. We have tried to measure f_0 and df_0/dz for the same kind of samples of different size and the same sample in the center and close to its edge. There are distinct change in f_0 but negligible variations in df_0/dz .

We also calculate f_0 as a function of the dielectric constant and thickness for thin films on a given substrate (see Fig.2). In this case, f_0 is no longer a linear function of the dielectric constant of films. Nevertheless, the dielectric constant of the film can be determined as long as df_0/dz is measured and the film thickness is given.

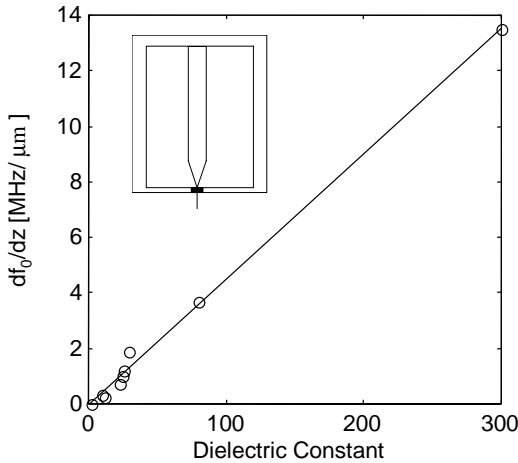


Fig. 1. Dependence of df_0/dz on dielectric constant of samples. The straight line is the theoretical calculation and the circles are experimental results measured on bulk crystals of different dielectric constants. The inset shows the coaxial $\lambda/4$ resonator used in our experiment

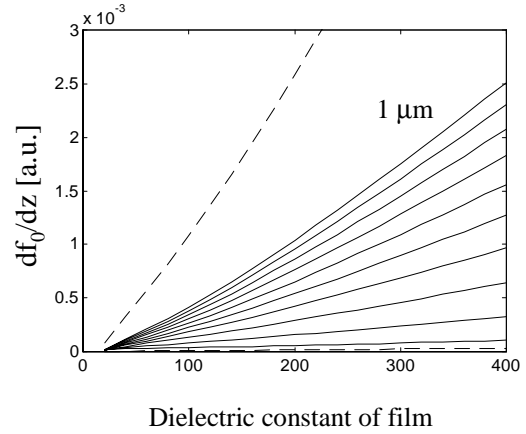


Fig. 2. Calculated df_0/dz as a function of dielectric constant for films grown on a substrate with $\epsilon=10$. The curves represent films with thicknesses ranging from 0 (bottom dashed line) to $1 \mu\text{m}$ (labeled line) in $0.1 \mu\text{m}$ steps. The top line (dashed) is for a film thickness of 0.5mm and represents the bulk value.

In the literature, there have been reports of nanometer-scale spatial resolution [1,3] and of 1 in 10^5 property sensitivity [1] in near-field microwave microscopies. However, high spatial resolution and high sensitivity have not been obtained simultaneously. Our calculation shows that for a cylindrical impurity of $\epsilon=120$ imbedded in a surrounding of $\epsilon=80$, the shift in the resonant frequency decreases with the size of the impurity and goes below the detection limit of 10^{-5} when the impurity is smaller than $1\mu\text{m}$. When the size of impurity is fixed, the shift of f_0 increases with contrast in permittivities as expected.

To determine material properties accurately, it is highly desired to obtain the topo-

graphic features and the dielectric properties simultaneously so that the contributions of topography can be excluded. [4,5] We have successfully obtained both in the measurement of a PbTiO_3 crystal by moving the tip vertically at various horizontal positions and measuring df_0/dz of the sample. Fig.3 shows the dependence of f_0 on tip-sample distance when the tip is above an a domain (circles) and a c domain (stars), respectively (df_0/dz drops to zero at touching).

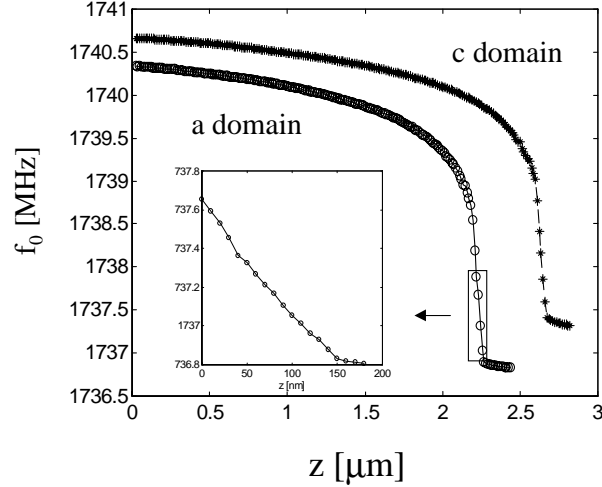


Fig. 3. Changes of f_0 with tip-sample distance for a (circles) and c (stars) domains in a PbTiO_3 crystal. The inset shows the dependence of f_0 on z close to the sample.

Fig.4 shows the simultaneously obtained f_0 , Q and topography of the PbTiO_3 crystal. The data show that the crystal consists of parallel a and c domains. The a domains have a higher dielectric constant ($\epsilon_a=105$) and a lower loss tangent ($\tan\delta_a=0.04$) than the c domains where ϵ_c and $\tan\delta_c$ are 35 and 0.08, respectively. [6]. As a result, f_0 is lower but Q is higher in the a domains. Because the domain wall forms an angle about 45° to the crystal surface, the peak of f_0 shifts to the left. The observed topography agrees with AFM results [7] and the bending angle between a and c domains is 3.8° , consistent with the theoretical prediction of 3.65° . [7,8] At the edge of the area under study, there is a small region, denoted by F in Fig.4(b), with much lower Q than the surroundings. This is due to defects in the crystal introduced during the growth process. In fact, we have found several such regions of various sizes and shapes.

We have measured $\text{Sr}_{1-x}\text{Ba}_x\text{TiO}_3$ films grown on MgO and LaAlO_3 substrates by pulsed laser deposition (PLD) process. [9] The image of as-deposited sample contains islands about $5\mu\text{m}$ in size. SEM and ANSOM measurements rule out surface roughness or grain size, since these features are smaller than 10 nm and 200 nm, respectively. [10] After annealing the sample at 1100°C for 6 hours, the film becomes much more uniform and the spatial variation in the permittivities at different regions is much smaller, as seen by comparing the scales in Fig.5(a) and (b).

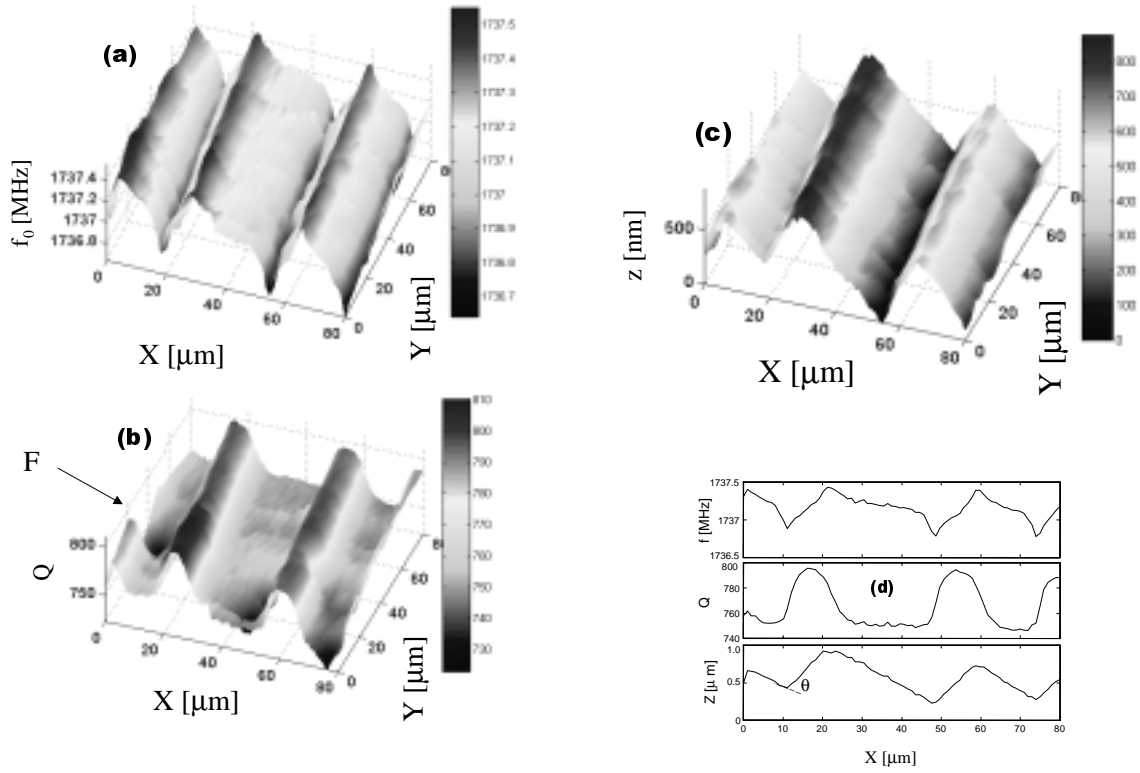


FIG. 4. Scanning-near-field images of a PbTiO_3 crystal showing (a) resonant frequency, (b) quality factor, (c) topography, and (d) a cross-section profile at $y=70 \mu\text{m}$. The angle θ denotes the bending at the a - c domain wall.

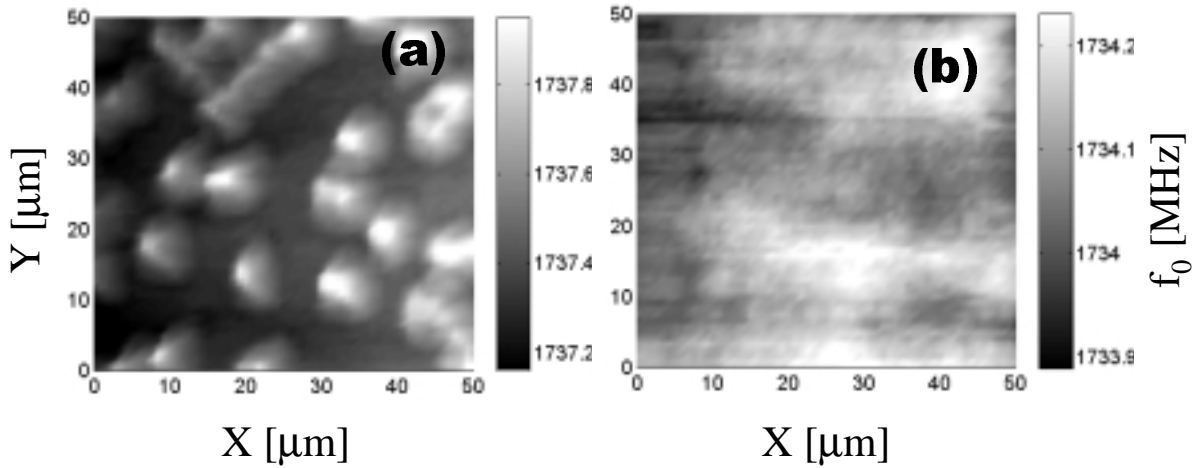


Fig. 5. Local variations of dielectric constants of $\text{Sr}_{1-x}\text{Ba}_x\text{TiO}_3$ films for (a) an as-deposited film and (b) a film annealed at 1100°C for 6 hours. The gray scale represents the measured resonant frequency.

IV. CONCLUSIONS

In summary, we have calculated the dependence of f_0 on material properties and parameters of the experimental setup. A linear dependence of df_0/dz on dielectric constant is found both experimentally and theoretically. In a PbTiO_3 crystal, the dielectric properties and topography are obtained simultaneously. For $\text{Sr}_{1-x}\text{Ba}_x\text{TiO}_3$ films, local variations for different processing conditions are observed. Future work will be focus on the accurate determination of loss in dielectric films.

Acknowledgements: The work is supported by DARPA. The authors would like to thank Dr. F. Rachford and Dr. J. Byers for helpful discussions.

-
- [1] C. Gao, X.D. Xiang, Rev.Sci.Instrum., **69**, 3846 (1998). Y. Lu, T. Wei, F. Duewer, Y. Lu, N.B. Ming, P.G. Schultz and X.D. Xiang, Science, **276**, 2004 (1997).
 - [2] D.E. Steinhauser, C.P. Vlahacos, F.C. Wellstood, S.M. Anlage, C. Canedy, R. Ramesh, A. Stanishevsky and J. Melngailis, Appl.Phys.Lett., **75**, 3180 (1999).
 - [3] Y. Cho, S. Kazuta and K. Matsuura, Appl.Phys.Lett., **75**, 2883 (1999).
 - [4] F. Duewer, C. Gao, I. Takeuchi, X.D. Xiang, Appl.Phys.Lett., **74**, 2696 (1999).
 - [5] C.P. Vlahacos, D.E. Steinhauser, S.K. Dutta, B.J. Feenstra, S.M. Anlage and F.C. Wellstood, Appl.Phys.Lett., **72**, 1778 (1997).
 - [6] A.V. Turik, Phys.Stat.Sol., **B94**, 525 (1979).
 - [7] Y.G. Wang, J. Dec and W.Kleemann, J.Appl.Phys., **84**, 6795 (1998).
 - [8] J.P. Remeika and A.M. Glass, Mater.Res.Bull. **5**, 37 (1970).
 - [9] W. Chang, J.S. Horwitz, A.C. Carter, J.M. Pond, S.W. Kirchoefer, C.M. Gilmore and D.B. Chrisey, Appl.Phys.Lett., **74**, 1033 (1999).
 - [10] C. Hubert and J. Levy, Appl.Phys.Lett., **73**, 3229 (1998).